ELSEVIER

Chemical Geology 161 (1999) 103–125

CHEMICAL GEOLOGY
INCLUDING
ISOTOPE GEOSCIENCE

www.elsevier.com/locate/chemgeo

The abundance of ^{13}C in marine organic matter and isotopic fractionation in the global biogeochemical cycle of carbon during the past 800 Ma

John M. Hayes [a,*], Harald Strauss [b,1], Alan J. Kaufman [c]

[a] Department of Geology and Geophysics, Woods Hole Oceanographic Institution, Woods Hole, MA 02543-1539, USA
[b] Institut für Geologie, Ruhr-Universität Bochum, Bochum 44780, Germany
[c] Department of Geology, University of Maryland, College Park, MD 20742, USA

Received 20 June 1998; accepted 22 October 1998

Abstract

New records of the abundance of ^{13}C in marine organic matter have been compiled for (i) the later Neoproterozoic, from 800 to 543 Ma (346 analyses), (ii) the Cambrian through the Jurassic (1616 analyses), and (iii) the Cretaceous and Cenozoic (2493 analyses). Comparison of these to existing compilations of the abundance of ^{13}C in sedimentary carbonates has allowed development of a record of the isotopic fractionation ($\equiv \varepsilon_{TOC}$) accompanying the production and burial of organic material. Over time, globally averaged values of ε_{TOC} have fallen in three ranges: (i) greater than 32‰ and apparently indicative of significant inputs from sulfide-oxidizing or other chemoautotrophic bacteria, notably during late Proterozoic interglacials at 752, 740–732, and 623–600 Ma; (ii) between 28 and 32‰ and indicative of maximal fractionation of carbon isotopes by phytoplanktonic producers, during the Neoproterozoic from 800 to 750 and from 685 to 625 Ma and during the Phanerozoic up to the early Oligocene; and (iii) less than 28‰, probably reflecting a reduction of primary fractionation by some combination of low levels of CO_2, rapid rates of growth, and high ratios of cellular volume to surface area during Neoproterozoic glaciations (740, 720, and 575 Ma) and since the early Oligocene. Evidence of similar variations during the Ordovician and Gondwanan glaciations is absent. The decline in ε_{TOC} since the early Oligocene, from 30 to 22‰, has been nearly linear. The structure of the record of ε_{TOC} suggests that the maximal isotopic fractionation between dissolved CO_2 and primary biomass has consistently been 25‰. Overall, the records provide compelling evidence that values of ε_{TOC} have varied widely and that the long-term average fractionation is roughly 30‰. © 1999 Elsevier Science B.V. All rights reserved.

Keywords: Marine organic matter; Isotopic fractionation; 800 Ma

---

[*] Corresponding author. Tel.: +1-508-289-2585; fax: +1-508-457-2183; e-mail: jhayes@whoi.edu

[1] Present address: Geologisch-Paläontologisches Institut, Westfälische-Wilhelms-Universität Münster, Corrensstrasse 24, 48149 Münster, Germany.

0009-2541/99/$ - see front matter © 1999 Elsevier Science B.V. All rights reserved.
PII: S0009-2541(99)00083-2

1. Introduction

Isotopic compositions of reactants and products in the global carbon cycle respond to two mass-balance requirements:

$$\text{Total carbon entering atmosphere and hydrosphere} = \text{Total carbon being sequestered in sediments}, \quad (1)$$

$$^{13}\text{C entering atmosphere and hydrosphere} = {}^{13}\text{C being sequestered in sediments}. \quad (2)$$

Combining these yields:

$$\delta_i = f_o \delta_o + (1 - f_o)\delta_a, \quad (3)$$

where δ_i, δ_o, and δ_a are the isotopic compositions of incoming carbon and of organic and carbonate carbon immobilized in sediments, and f_o is the fraction of carbon that is buried in organic form. For any point in time, Eq. (3) can be usefully recast by defining ε_{TOC} as the average isotopic fractionation between total organic carbon (TOC) and sedimentary carbonates ($\approx \delta_a - \delta_o$), thus:

$$\delta_a = \delta_i + f_o \varepsilon_{TOC}. \quad (4)$$

For studies of the history of the carbon cycle, the process-oriented variables on which attention should logically be focused are f_o and ε_{TOC}. The first of these bears directly on the global redox balance and the second varies in response to evolutionary and environmental changes. Neither can be measured directly, particularly given the requirement for globally representative values. There are three basic problems: global averaging, reconstruction of δ_i, and the required comparison of δ_a and δ_o.

In practice, attention has been focused on records of δ_a. Since carbonate sediments monitor the isotopic composition of a reactant that is stirred globally (albeit imperfectly), averaging is less problematic. Since δ_a is linearly related to f_o (provided δ_i and ε_{TOC} are constant; a risky assumption to which Hayes, 1983; Kump, 1989; Raymo, 1997 have called attention), it is relatively rich in information. In a notable example of rigor, Derry and France-Lanord (1996) were able to deal explicitly with reconstruction of δ_i and with changing values of ε_{TOC} by restricting their attention to the Neogene.

Here, we ask two questions. First, has ε_{TOC} varied significantly over the last 800 Ma? Second, if so, what evolutionary and paleoenvironmental information might those variations provide? We have compiled reports of the carbon-isotopic compositions of sedimentary organic matter (thus following Degens, 1969; Welte et al., 1975; Hayes et al., 1983; Lewan, 1986). By comparing these to previously established records of δ_a, we have developed an 800-Ma record of ε_{TOC}. With the aims of focusing on the most important component of sedimentary organic carbon and of obtaining a record that could be considered in terms of the processes leading to its development, we have considered only marine sediments and organic materials of marine origin. For the most accurate reconstruction of global geochemical budgets, it will be necessary to consider *all* organic carbon that are immobilized in sediments, specifically including terrigenous inputs to marine sediments and all components of freshwater sediments. If these are abundant enough, and if their isotopic compositions differ significantly from those of marine materials, adjustments to the record of ε_{TOC} will result.

As fundamental data, we recommend maintenance and refinement of records of δ_a and δ_o and development of estimates of δ_i. For discussion and interpretation, we recommend attention to records of f_o and ε_{TOC} or δ_a and ε_{TOC}. Separate attention to δ_o should be avoided, since δ_o both rides up and down with δ_a (thus carrying a redundant signal component) *and* responds to changes in ε_{TOC}.

2. Data and calculations

2.1. Time scales

The time interval considered here begins 800 Ma ago, during the Neoproterozoic, and extends to the Holocene. In compiling records and estimating the ages of sedimentary beds, the dates summarized in Table 1 have been used. Methods used for adjustment of ages previously referred to other time scales are described in the sections below.

Table 1
Ages used in compilation of the present isotopic records

Event or time interval	Age (Ma)	References
Cenozoic		Berggren et al. (1995)
Paleozoic and Mesozoic not otherwise specified		Harland et al. (1990)
Arenig–Llanvirn (early–middle Ordovician) boundary	465	Young and Laurie (1996)
Cambrian–Ordovician boundary	490	Young and Laurie (1996)
St. David's–Merioneth (middle–late Cambrian) boundary	500	Young and Laurie (1996)
Caerfai–St. David's (early–middle Cambrian) boundary	509	Young and Laurie (1996)
Nemakit–Daldyn–Tommotian boundary	534	see Kaufman et al. (1996)
Precambrian–Cambrian boundary	543	Bowring et al. (1993), Grotzinger et al. (1995)
Start of negative excursion of δ_a prior to PC–C boundary	544	Pelechaty et al. (1996)
End of latest Vendian positive excursion of δ_a	549	Grotzinger et al. (1995)
Minimum δ_a, second Varanger ice age	575	Saylor et al. (in press)
Minimum δ_a, first Varanger ice age	590	Saylor et al. (in press)
Minimum δ_a, second Sturtian ice age	720	[a]
Minimum δ_a, first Sturtian ice age	740	[a]
Base of Shaler and Veteranen Groups	800	[b]

[a] Maximum age of lower tillite is 746 ± 2 Ma (Hoffman et al., 1996). Ages of 740 and 720 Ma are estimates (nb, on carbon-isotopic evidence, upper tillite is distinct from Varangian units (see Kaufman et al., 1991; Smith et al., 1994; Kaufman and Knoll, 1995).

[b] Shaler is older than 723 ± 3 Ma (Heaman and Rainbird, 1990), and C and Sr isotopic correlations (Knoll et al., 1986; Asmerom et al., 1991; Kaufman and Knoll, 1995) indicate that its Kilian Fm. is equivalent to the lower Svanbergfjellet Fm of the Veteranen Group and to the Chuos (lower Sturtian) diamictite in Namibia. Basal age of 800 Ma is an estimate.

2.2. Values of δ for organic and carbonate carbon

Assessment of ε_{TOC} requires knowledge of both δ_a and δ_o. Accordingly, it has been necessary not only to compile results of isotopic analyses of organic carbon but also to compile or to select isotopic records for carbonate carbon.

2.2.1. Neoproterozoic

Sources of data, locations, and time intervals are summarized in Table 2. The investigations yielding these results have been stratigraphically oriented. Consequently, (i) systematic relationships between age and position in the section are specified in each report and (ii) sampling has been concentrated at time horizons of particular interest. To deal with the resulting highly variable temporal resolution, we have combined the data from all sections, sorted points according to assigned age, and computed moving-average values of δ_o and δ_a. To begin, 25-sample groups ($n = 56$) were examined. Of 1400 samples, 409 had yielded values for both δ_o and δ_a, 885 contained analyzable concentrations only of carbonate, and 106 had yielded values only for δ_o.

As noted in Table 2, dolomitic samples are abundant in these Precambrian sections, and lithologies have been consistently specified along with the isotopic compositions. There were 52 25-sample groups in which the mean δ value of at least three limestones could be compared to that of at least three dolomites. In 16 of these, the carbon-isotopic difference between calcite and dolomite was significant at the 95% confidence level (12 with dolomite depleted in ^{13}C relative to limestone, four vice versa). Such differences could reflect significant secular changes in δ that happened to be correlated with global variations in the abundances of dolomite and calcite within the time span of a 25-sample block. The overall average limestone–dolomite difference was 0.59‰, with dolomites being depleted in ^{13}C relative to limestones. The standard deviation of the population of differences ($n = 52$) was 1.77‰. Conceivably, a ‘‘correction’’ might have been applied with, e.g., 0.6‰ being added to the δ values of all dolomites. However, since the 95% confidence interval for that correction would be ±0.5‰, the drawbacks of dealing with adjusted data were considered greater than any benefits. The values of δ_a reported

Table 2
Sources of δ values for samples of Neoproterozoic age

Unit or location	Age (Ma)		Number of δ_a values		Number of δ_o values		References[c]
	Top	Bottom	Lms[a]	Dol[b]	Lms[a]	Dol[b]	
Kotuikan River, Siberia	536	544	47	84			9,10
Kytyngeder River, Siberia	544	548		32			11
Chekurov anticline, Siberia	544	550	74	62			11
Oolohan Ooekhtekh River, Siberia	545	552		44			11
Olenek River, Siberia	543	552		42			11
Khorbosuonka River, Siberia	538	553	51	36	35	16	8
Nama Group, southern Namibia	544	560	195	18	46	7	3,4,6,14
Witvlei Group, central Namibia	555	589	10	34	5	7	3,4,14
East Greenland	554	735	26	10	32	8	1
Mackenzie Mountains, NWT, Canada	543	750	86	29	70	25	5,12
Otavi Group, northern Namibia	589	766	62	158	33	83	3,13
Nordauslandet	575	780	7	14	27	13	1
Shaler Group, Victoria Island, Canada	740	800	48	52	24	20	7
Spitsbergen	555	800	39	57	42	28	1,2,4,12

[a] Limestones.
[b] Dolomites.
[c] 1: Knoll et al. (1986); 2: Fairchild and Spiro (1987); 3: Kaufman et al. (1991); 4: Derry et al. (1992); 5: Narbonne et al. (1994); 6: Grotzinger et al. (1995); 7: Kaufman and Knoll (1995); 8: Knoll et al. (1995a); 9: Knoll et al. (1995b); 10: Kaufman et al. (1996); 11: Pelechaty et al. (1996); 12: Kaufman et al. (1997); 13: Hoffman et al. (in press); 14: Saylor et al. (in press).

here represent averages in which samples have been combined without regard to lithology.

Values of δ_o could be compared among at least three dolomitic and three calcitic samples in 27 of the 56 blocks. Significant differences were found in eight of these, with organic material in dolomites being enriched in ^{13}C relative to that in limestones in five cases. The overall average difference was 0.90‰, with organic carbon in dolomites tending to be enriched in ^{13}C. Although this is larger than the difference observed for carbonates, the standard deviation of the population of differences ($n = 27$) is 4.35‰. The average difference is therefore significant only at the 30% confidence level and no adjustment or ''correction'' can be justified.

When the 25-sample average was advanced in five-sample steps, the time equivalent to each step averaged 0.9 Ma and ranged from 0.02 to 9 Ma. On average, each group contained 23.1 values of δ_a and 9.5 values of δ_o (ranges 5–25 and 0–23, respectively). The resulting record of δ_a is displayed in subsequent sections of this report. The corresponding record of δ_o, however, was noisy and, in some time intervals, the density of values for δ_o was too sparse to support 25-sample averaging. The noise was traced to a systematic enrichment of ^{13}C in organic material from the Nama and Otavi Groups (Kaufman et al., 1997). Whenever δ_o values from either of these units were abundant, the average value of δ_o for a 25-sample group would be shifted upward from the trend based on all other units (i.e., organic carbon in the Nama and Otavi Groups is enriched in ^{13}C relative to that in coeval samples from other locations). This systematic enrichment could be due either to conditions in the depositional environment or to the effects of post-depositional heating. Resolution of that question is a subject for further research. Here, because of the marked contrast with all other units, because many samples displayed δ_o values that are usually characteristic of thermally altered materials (i.e., $-16 < \delta_o < -7$‰; see Hayes et al., 1983), and because the sampled successions from the Otavi Group, at least, have reached the lower greenschist facies of metamorphism (P.J. Hoffman, personal communication), all δ_o values from the Nama and Otavi Groups were excluded from further consideration.

To develop a record of the isotopic composition of organic carbon, groups with varying numbers of samples were defined so that each contained 15 values of δ_o. When this ''15-organic'' average was advanced so that each step was large enough to cover five samples for which δ_o was known, 69 group-average values of δ_o were obtained. The time equivalent to each step averaged 3.6 Ma and ranged from 0.6 to 22 Ma. All groups contained exactly 15 values for δ_o, but the number of values of δ_a in each group ranged from 6 to 257, depending on the distribution of analyses, and averaged 56. The record of δ_a values obtained in this way is not shown here, but its major features did not differ from those of the 25-sample moving average described in the preceding paragraph.

2.2.2. Cambrian through Jurassic

The 1616 values of δ_o were collected from the literature, from unpublished reports, and from personal communications. These include results of analyses of separated kerogen and of TOC present in whole rock samples of various lithologies. Samples were excluded if independent evidence indicated that post-depositional effects had been severe enough to alter isotopic compositions (cf. Strauss et al., 1992). This pertains particularly to effects associated with thermal alteration, as indicated, e.g., by H/C ratios. Similarly, samples were excluded if independent evidence indicated that organic material was clearly of terrestrial origin or if the isotopic composition of the material had been significantly affected by admixture of allochthonous material. Where available, this information has been derived from rock-eval data and/or from analyses of macerals.

Age constraints vary significantly. In 25 cases, stratigraphic position could be specified in terms of stage (roughly, ±2 Ma). In 26 cases, stratigraphic position was reported or could be determined in terms of epoch (±6 Ma). For 30 reports, it was possible only to assign the observed values of δ_o to a particular period (±20 Ma or more). With this limitation in mind, mean ages have been assigned to each stratigraphic unit and individual values of δ_o within each 10-Ma window (520–510, 510–500, etc.) have been averaged, resulting in 26 10-Ma means for the time interval from the early Cambrian to the latest Jurassic (there being 13 10-Ma intervals lacking any reports of δ_o).

The isotopic record used for carbonate carbon is the 20-Ma moving average shown as Fig. 10 by Veizer et al. (this volume), with ages in the Cambrian and earliest Ordovician adjusted to the time scale specified in Table 1. For each interval, the standard deviation is determined from the range required to include 68% of the observations (Veizer et al., this volume).

2.2.3. Cretaceous and Cenozoic

Results of 2493 analyses of the isotopic composition of sedimentary organic carbon of marine origin were obtained almost entirely from reports of the Deep Sea Drilling Project and the Ocean Drilling Program. The composition of this collection is summarized in Table 3. Samples were excluded if the organic material was described as being of terrigenous origin, if the hydrogen index (when available) was lower than 50 mg hydrocarbons/g organic carbon (thus strongly indicating alteration or reworking), or if the total concentration of organic carbon was less than 0.1% (a circumstance often leading to inaccurate results in survey procedures). For each sample, the stratigraphic assignment noted in the report of the isotopic analyses, often based on a preliminary assessment, was checked against the stratigraphy described in the final, definitive report for the hole. When these assignments were inconsistent, precedence was given to the assignment in the final report.

To estimate mean values of δ_o for each of the intervals listed in Table 3, (i) the average value of δ_o at each site was determined; (ii) a weighting factor between 1 and 5 was assigned to each of those averages; and (iii) an overall weighted mean was computed. For each site, the weighting factor was based on the number of analyses, the estimated reliability of the results, and the stratigraphic distribution. To provide some examples, the average of five or more highly reliable analyses widely distributed throughout the stratigraphic interval would be assigned a weighting factor of 5 and the average of tens of analyses obtained using a survey procedure and tightly grouped within a few core segments would be assigned a weighting factor of three. This procedure avoids attributing undue weight to densely sampled intervals or to results of reconnaissance analyses.

To facilitate investigation of possible latitudinal effects on δ_o, assistance was generously provided by Dr. David Rowley of the paleogeography research group at the University of Chicago, who determined

Table 3
Sources and distribution of isotopic analyses of organic carbon, samples of Cretaceous and Cenozoic age

Interval	Age (Ma)	Number of sites	Weighted average paleolatitude	Number of analyses	References[a]
Pleistocene	0.9	15	30.3	221	2,12,17,19,22,23,25,26
Pliocene	3.5	16	38.8	1045	2,7,15–19,22,23,25,26
Late Miocene	8.3	12	44.4	129	6,7,12,16–18,22,23
Middle Miocene	13.8	15	37.3	228	2,6,7,9,12,15,16,18,22,23,25
Early Miocene	20.1	12	36.9	91	2,6,7,9,12,15,16,18,23,25
Late Oligocene	26.2	8	44.4	140	2,6,7,12,18,23
Early Oligocene	31.1	2	56.1	111	17,18
Late Eocene	35.3	4	44.5	27	2,6,18,21
Middle Eocene	43.0	7	43.8	33	2,6,7,10,12,16,18
Early Eocene	51.9	5	34.1	8	6–8,10,11
Late Paleocene	57.9	3	43.1	62	10,12,18
Early Paleocene	63.0	3	27.7	3	7,8,12
Maastrichtian	69.5	2	42.2	3	7,20
Campanian	78.5	1	1.7	2	1
Santonian	84.8	3	46.6	5	2,4,20
Coniacian	87.6	2	51.3	14	2,20
Turonian	89.5	6	31.7	99	4,7,8,13,20
Cenomanian	93.7	8	26.2	54	4,5,8,12,13,20,21,27
Albian	104.5	8	27.7	107	2,3,5,12,14,20,21,27
Aptian	118.3	3	35.9	13	5,7,12
Barremian	128.2	2	31.3	16	4,5
Hauterivian	133.4	6	21.8	37	4,5,12,21,24,27
Valanginian	137.9	7	27.4	40	4,5,12,21,24,27
Berriasian	143.2	4	25.9	5	5,12,27

[a] 1: Buchardt and Holmes (1995); 2: Calder et al. (1974); 3: Dean (1981); 4: Dean and Arthur (1987); 5: Dunham et al. (1988); 6: Erdman and Schorno (1978a); 7: Erdman and Schorno (1978b); 8: Erdman and Schorno (1978c); 9: Erdman and Schorno (1978d); 10: Erdman and Schorno (1979a); 11: Erdman and Schorno (1979b); 12: Galimov et al. (1980); 13: Hayes et al. (1989); 14: Katz (1988); 15: Kennicutt et al. (1985); 16: Lewan (1986); 17: Macko (1989); 18: Macko and Pereira (1990); 19: Muzuka et al. (1991); 20: Nohara et al. (1984); 21: Patton et al. (1984); 22: Romankevich et al. (1980); 23: Schorno (1980); 24: Schorno and Erdman (1980); 25: Simoneit and Mazurek (1981); 26: Simoneit et al. (1984); 27: Thompson and Dow (1990).

paleocoordinates for each δ_o value (i.e., the paleolatitude and paleolongitude for each site during each stratigraphic interval from which organic carbon had been analyzed). This information has been used in two ways. First, in order to provide an overview of the data set, a weighted-average paleolatitude has been computed for each stratigraphic interval:

$$\text{Weighted-average paleolatitude} = \Sigma(w_i L_i)/\Sigma w_i, \tag{5}$$

where the w_i values are the weighting factors described above and the L_i terms are absolute values of paleolatitudes (i.e., samples from 45°N and 45°S would yield an average of 45°, not zero). Results are shown in Table 3. Second, as described in Section 3, samples with high paleolatitudes were excluded during some trial calculations.

The record of δ_a values for the Berriasian through the Santonian stages of the Cretaceous is based on that provided by Arthur et al. (1985b). This is closely similar to the record developed by Veizer et al. (this volume) except that its Aptian–Albian isotopic peak is broader. Values for the Campanian and Maastrichtian stages are from the latter record. For the Cenozoic, we have adopted the bulk-sediment record provided by Shackleton (1987).

2.3. Calculations

2.3.1. Availability of numerical results

Point lists for all graphs, including numerical results of the calculations outlined below and related uncertainties, can be downloaded from http://www.nosams.whoi.edu/jmh.

2.3.2. Carbon-cycle descriptors

The isotopic fractionation between carbonate carbon and organic carbon is expressed in terms of ε_{TOC}. When both ε and δ are expressed in units of per mil:

$$\varepsilon_{TOC} \equiv 10^3(\alpha_{TOC} - 1) = 10^3\{[(\delta_a + 1000)/(\delta_o + 1000)] - 1\}. \qquad (6)$$

For the Neoproterozoic, the values of δ_a and δ_o were those determined using the ''15-organic'' moving average described above. For the Cambrian–Jurassic time interval, values of δ_a were obtained from the 20-Ma moving average described by Veizer et al. (this volume) and values of δ_o were averages for 10-Ma windows as described above. For the Cretaceous and Cenozoic, values of δ_a and δ_o were averages for the intervals noted in Table 3.

Rearrangement of Eq. (3) yields an expression for f_o and thus would provide a means of monitoring changes in the relative rates of burial of carbonate and organic carbon *if* values of δ_i were known. Here, values of f_o for each stratigraphic interval have been estimated from:

$$f_o = (\delta_a + 5)/(\delta_a - \delta_o), \qquad (7)$$

i.e., we have set $\delta_i = -5‰$ and thus adopted the ''first approximation'' utilized by Derry and France-Lanord (1996), in which it is assumed that δ_i will be equal to the average δ value of total sedimentary carbon (Holser et al., 1988). Since it takes into account variations in ε_{TOC}, the resulting record is one step closer to the process of carbon burial than is a record of δ_a.

2.3.3. Assessment of uncertainties

It is possible to discuss systematically only uncertainties associated with the scatter of the values of δ_a and δ_o that provide the basis for these records. To these must be added some consideration of inadequacies in sampling. For older units, open-ocean samples are rare to nonexistent. For all units, sampling reflects a variety of biases imposed by the interests of the original investigators and by the methods of collection employed here. Publication of the present records — to be followed, no doubt, by recognition of their imperfections — is an initial step towards the reduction of those uncertainties.

Because accidental biases and incompleteness are probably the most important uncertainties bearing on the records constructed here, and in order to allow compact and uncluttered graphic presentation of the records, neither error bars nor distributional envelopes are shown in the figures. However, the magnitudes of these uncertainties are summarized quantitatively below and the specific, point-wise estimates of uncertainty can be downloaded from the web site noted above.

For the Neoproterozoic, calculation of standard deviations for the populations of individual values of δ_a and δ_o within each ''15-organic'' group was straightforward. Results are summarized in Table 4.

Table 4
Standard deviations

Parameter	Age range[a]	Standard deviation[b]		
		Average	Minimum	Maximum
δ_a, Population	NP	2.5	0.8	4.5
	C–J	1.3	0.3	2.6
	K–Cen		[c]	
δ_o, Population	NP	3.1	1.0	4.8
	C–J	1.5	0.07	2.8
	K–Cen	1.5	0.1	3.5
δ_a, Group mean	NP	0.4	0.07	1.6
	C–J		[d]	
	K–Cen	0.3	0.1	0.6
δ_o, Group mean	NP	0.8	0.3	1.2
	C–J	0.2[e]	0.05[e]	0.6[e]
	K–Cen	0.8	0.1	2.6
ε_{TOC}	NP	1.0	0.5	1.8
	C–J	1.5	0.3	2.9
	K–Cen	0.9	0.3	2.6
f_o	NP	0.06	0.05	0.08
	C–J	0.05	0.05	0.06
	K–Cen	0.06	0.05	0.07

[a] NP, Neoproterozoic; C–J, Cambrian–Jurassic; K–Cen, Cretaceous–Cenozoic.

[b] Standard deviations varied in response to the scatter and number of points within each age interval. The minima and maxima tabulated here indicate the range of that variation.

[c] Not reported by initial investigators. Standard deviations of mean values, required for error-propagation calculations, were estimated. See text.

[d] Numbers of observations were not reported by initial investigators, thus standard deviations of mean values could not be computed. See text regarding error-propagation calculations.

[e] Low values result from large numbers of observations. See text regarding error-propagation calculations.

These measures of spread in the distributions reflect the combined effects of analytical imprecision, natural variability at any given time horizon, and secular change within the time interval covered by the sample group. Since values of $\varepsilon_{\mathrm{TOC}}$ and f_{o} are based on average values of δ_{a} and δ_{o}, standard deviations of these means ($\equiv \sigma/n^{1/2}$) are also shown in Table 4.

For Cambrian to Jurassic ages, standard deviations of populations of δ_{a} values within each 20-Ma span were provided by Veizer et al. and are summarized in Table 4 (δ_{a}, population, C–J) along with corresponding values for δ_{o} populations within each 10-Ma window. As indicated by the low standard deviations, the processes of selection employed in construction of the δ_{a} record yielded relatively tight distributions. If these already-low uncertainties were reduced by substantial factors (i.e., $n^{1/2}$) in order to estimate the standard deviation of the mean value, it would have the effect of postulating a surface ocean with perfect isotopic homogeneity (since the standard deviation represents natural as well as analytical variability). A similar problem arises with the standard deviation of the mean value of δ_{o}, for which the very large values of n within each stratigraphic interval led to the very low values shown in Table 4 (δ_{o}, group mean, C–J). To avoid development of artifactually low uncertainties for $\varepsilon_{\mathrm{TOC}}$ and f_{o}, alternative values were used in error-propagation calculations, as described below.

For stratigraphic intervals in the Cretaceous and Cenozoic, standard deviations of populations of site-average values of δ_{o} varied as noted in Table 4. Standard deviations of weighted-mean values of δ_{o} (Table 4), used in error-propagation calculations, were computed from $(5\sigma^2/N)^{1/2}$, where σ is the standard deviation of the population of site averages and N is the sum of the weighting factors. Standard deviations for mean values of δ_{a} (Table 4) were estimated from the extent of agreement between the older records (Arthur et al., 1985b; Shackleton, 1987) and that of now developed by Veizer et al. (this volume), and were increased where secular changes within a particular stratigraphic interval were large.

In estimates of the propagation of errors, the uncertainty in $\varepsilon_{\mathrm{TOC}}$ has been computed from:

$$\sigma_{\varepsilon}^2 \approx \sigma_{\mathrm{a}}^2 + \sigma_{\mathrm{o}}^2, \tag{8}$$

where σ_{a} and σ_{o} are the standard deviations of mean values of δ_{a} and δ_{o} as identified in the preceding sections and summarized in Table 4. For stratigraphic intervals of Cambrian-to-Jurassic age, σ_{a} was approximated by $\sigma/4$, where σ is the standard deviation of the population of individual values of δ_{a} for that interval, and σ_{o} was set equal to the standard deviation of the population of individual δ_{o} values. As shown in Table 4, the resulting estimates of σ_{ε} are roughly equal to those obtained for the other age intervals. This treatment of the C–J interval is justified because (i) the standard deviation of the population of δ_{a} values has been systematically minimized through selection of exceptionally preserved samples and (ii) the large values of n characteristic of averaging across all analyses (as opposed to averaging across sites, as in the Cretaceous and Cenozoic) would have the effect of unrealistically minimizing σ_{o}.

An estimate of the standard deviation of f_{o} would be provided by:

$$\sigma_{\mathrm{f}}^2 = \left(\sigma_{\mathrm{a}}^2 + \sigma_{\mathrm{i}}^2\right)/D^2 + \left[(\delta_{\mathrm{a}} - \delta_{\mathrm{i}})/D^2\right]^2\left(\sigma_{\mathrm{a}}^2 + \sigma_{\mathrm{o}}^2\right), \tag{9}$$

where values of σ_{a} and σ_{o} are as specified above and, for convenience in notation, $D \equiv \delta_{\mathrm{o}} - \delta_{\mathrm{a}}$. Calculation of σ_{f} thus requires values for δ_{i} and σ_{i}, the isotopic composition of carbon entering the atmosphere and hydrosphere and the uncertainty in that value. Here, we have adopted $\delta_{\mathrm{i}} = -5‰$ and $\sigma_{\mathrm{i}} = 1.5‰$. In fact, however, δ_{i} has surely not been constant, and the uncertainty about its value — or the magnitude of its natural variations — also varies in response to tectonic factors.

3. Results and discussion

Records of isotopic abundances, of the overall fractionation of ^{13}C in the carbon cycle, and estimates of variations of f_{o} are shown in Figs. 1–3.

3.1. Assessment of the records

3.1.1. Neoproterozoic

The records shown in Fig. 1 indicate that isotopic fractionation varied widely during the Neoproterozoic. Significant declines in both isotopic fractionation and the burial of organic carbon relative to carbonate carbon are associated with the first and second Sturtian glaciation, with the second Varanger glaciation, and with an isotopic event at the Precambrian–Cambrian boundary for which evidence of glaciation is lacking (Kimura et al., 1997; Bartley et al., 1998 but see also Bertrand-Sarfati et al., 1995). Isotopic fractionation declined only slightly during the first Varanger glaciation, but (if the estimate based on $\delta_i \approx -5‰$ is indicative) that event is marked by a strong decline in the relative rate of burial of organic carbon. Comparisons to Figs. 2 and 3 show that, outside of the glaciations, the rate of burial of organic carbon *relative to* that of carbonate carbon was significantly higher than that characteristic of the Phanerozoic (as noted already during numerous considerations of the record of δ_a, e.g., Knoll et al., 1986; Derry et al., 1992; Kaufman and Knoll, 1995).

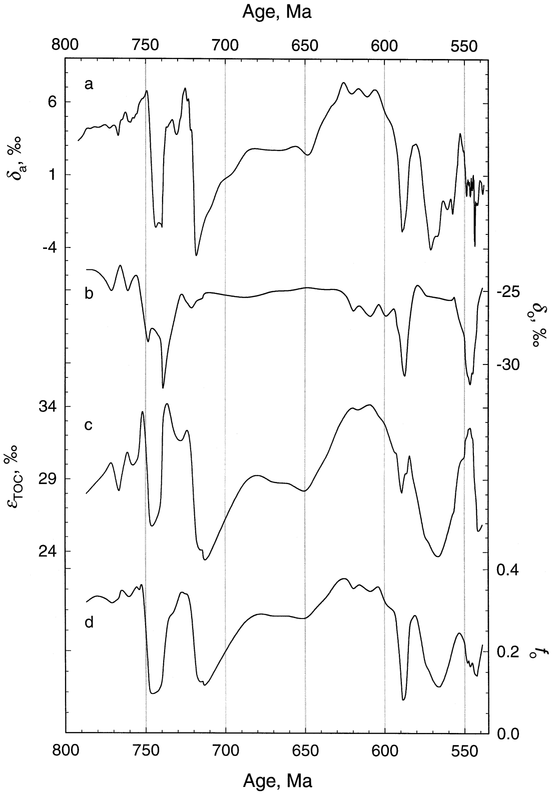

Fig. 1. Neoproterozoic records. (a) 25-Sample, moving-average isotopic compositions of carbonates. (b) 15-Sample, moving-average isotopic compositions of TOC in sedimentary rocks. (c) The corresponding isotopic fractionation between carbonate and TOC. (d) Estimated values of f_o, the fraction of carbon being buried in organic form. Sources of data, calculations, and estimates of uncertainty are described in the text and in Tables 2 and 4. Detailed data in tabular form, including pointwise estimates of uncertainty, can be obtained from http://www.nosams.whoi.edu/jmh.

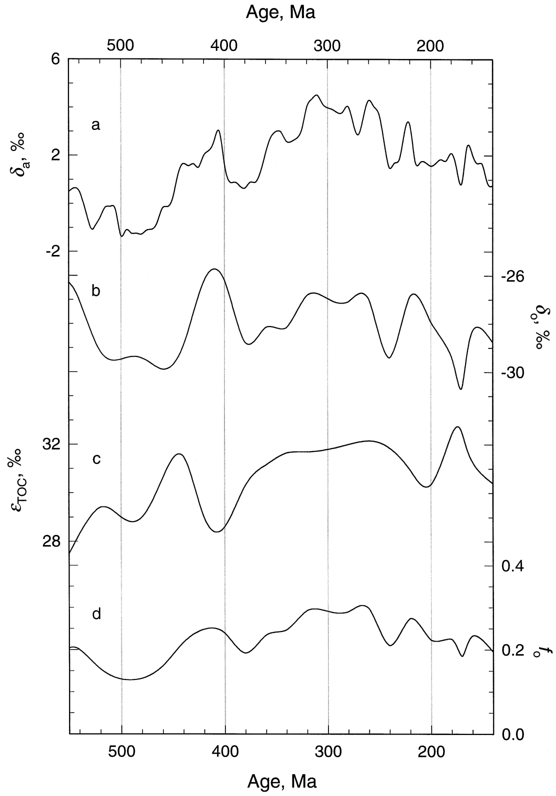

Fig. 2. Cambrian–Jurassic records. (a) 20-Ma moving average (5-Ma steps) of isotopic compositions of carbonates (Veizer et al., this volume). (b) A manually smoothed representation of 26 10-Ma average values for the isotopic composition of organic carbon. The method of age assignments described in the text resulted in no values for the 10-Ma increments centered on 505, 485, 465, 405, 335, 325, 315, 295, 285, 275, 235, 215, and 205 Ma. (c) The corresponding isotopic fractionation between carbonate and TOC. (d) Estimated values of f_o, the fraction of carbon being buried in organic form. Calculations are described in the text of this report and uncertainties are summarized in Table 4. Detailed data in tabular form, including unsmoothed averages and pointwise estimates of uncertainty, can be obtained from http://www.nosams.whoi.edu/jmh.

Uncertainties are associated with the method used to estimate values of ε_{TOC}. To recapitulate briefly: (i) samples were sorted in order of *assigned* age,

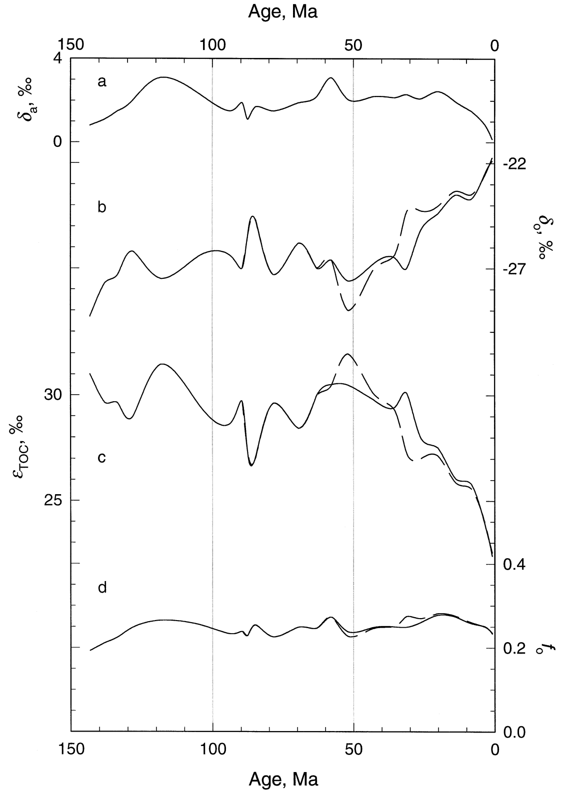

Fig. 3. Cretaceous and Cenozoic records. (a) Isotopic compositions of carbonates, as described in text. (b) Average isotopic compositions of TOC for time increments and data sources identified in Table 3. Broken line indicates record that excludes all points from paleolatitudes greater than 45°. (c) The corresponding isotopic fractionations (i.e., with and without exclusion of high-latitude data) between carbonate and TOC. (d) Estimated values of f_o, the fraction of carbon being buried in organic form. Calculations are described in the text of this report and uncertainties are summarized in Table 4. Detailed data in tabular form, including pointwise estimates of uncertainty, can be obtained from http://www.nosams.whoi.edu/jmh.

thus producing a sequence in which samples from different tectonic provinces were interspersed; and (ii) values of δ_a and δ_o were compared among samples with closely similar ages, *without regard for location*. Thus, the isotopic composition of a carbonate from the Shaler Group (Victoria Island) might be compared with that of organic material from the Veteranen Group (Svalbard). The validity of this approach depends on the accuracy of the age assignments that guide the comparisons. Correlations between Precambrian sedimentary successions are often profoundly uncertain, and special consideration of the problem is required here because the carbonate-isotopic records have themselves been used in establishing the relationships underlying the age assignments. These ‘‘ages’’ are, therefore, more properly viewed as parameters within a stratigraphic model.

A question then arises: Is it possible that undetected errors in the age assignments are responsible for the structure in the record of ε_{TOC}, and that perfectly correct correlations would erase or greatly alter that structure? An answer can be based on the subset of observations of ε_{TOC} for which there is no possibility of errors in age assignments, namely those cases in which both δ_a and δ_o have been measured in the same physical sample. If these single-sample values are assigned the symbol ε_{pair}, they can be compared to values of ε_{TOC} estimated from the group-average values of δ_a and δ_o. The latter define the trend line shown as Fig. 1c and can be assigned the symbol ε_{trend}. If ε_{trend} is responding faithfully to global variations in the average value of ε_{TOC}, we expect $\varepsilon_{pair} \approx \varepsilon_{trend}$ wherever these values can be compared. For the 246 cases in which values of both δ_a and δ_o were determined from the same sample, the average value of $\varepsilon_{trend} - \varepsilon_{pair}$ is 0.16‰, indicating either that ε_{trend} is accurately reflective of variations in fractionation or that errors have cancelled fortuitously. When ε_{trend} is plotted vs. ε_{pair}, the slope of the major axis is 0.67, indicating — as would be expected, given the extensive use of averaging in derivation of the trend line — that pointwise variations measured by ε_{pair} tended to exceed those represented by the trend line. The correlation coefficient, r, is significant at the 99% confidence level, but the magnitude of r^2 is relatively low, indicating that only 28% of the variation in ε_{pair} is explained by variations in ε_{trend} and leaving the remainder to analytical, environmental, and stratigraphic ‘‘noise’’. These factors would include analytical errors, site-specific effects on the magnitude of ε_{TOC} (as are frequently observed in modern environments), and errors in correlation. These comparisons of ε_{pair} and ε_{trend} suggest that the trend line in Fig. 1c is unbiased in the sense that it is not systematically high or low, and conservative in that it is unlikely to overestimate variations in ε_{TOC}. They indicate also that there is much room for improvement in detail and that only the most fundamental features of the record may prove to be robust.

3.1.2. Cambrian through Jurassic

In contrast to the much more severe Neoproterozoic glaciations, the records shown in Fig. 2 provide no evidence for declines in fractionation during the late Ordovician (ca. 440 Ma) and Gondwanan (250–320 Ma) glaciations. Values of ε_{TOC} are close to those observed during non-glaciated portions of the Neoproterozoic and significantly greater than the value of 25‰ employed in many models of the Phanerozoic carbon cycle. Relative rates of burial of organic carbon (i.e., values of f_o) were especially low during the Cambrian and, as noted from mass balances based on carbonate-isotopic evidence (e.g., Berner, 1994), were at Phanerozoic maxima during the Permian and Carboniferous periods.

Uncertainties are associated with problems of temporal resolution and with spotty sampling. Ironically, problems with age assignments are greater for the Cambrian–Jurassic time interval than for its older and younger counterparts. For the Neoproterozoic, a strong interest in the use of carbon-isotopic records as a means of stratigraphic correlation has provided records that are relatively continuous and well-ordered. For the Cretaceous and Cenozoic, the stratigraphic information available from ocean-drilling records provides good control. Neither of these advantages pertains to the Paleozoic and Mesozoic, where richness of the fossil record obviates any need for correlations based on carbon-isotopic records and where sampling and reporting have not been as systematic as that engendered by the ocean-drilling projects. Here, for each 10-Ma interval in which an average value of δ_o was obtained, values of ε_{TOC} and f_o have been calculated as described in the discussions of Eqs. (6) and (7). From the resulting points, a smooth curve, shown in Fig. 2c, was then drawn to represent the trend of values of ε_{TOC}. The trend lines shown in Fig. 2b and d for values of δ_o and f_o are based on the lines for δ_a and ε_{TOC}. The stratigraphic imprecision thus imposed on the record of δ_o undoubtedly obscures some features that will become visible in better records, a probable example being the rapid decrease in δ_o which is visible in some Permian–Triassic boundary sections that have been continuously sampled and analyzed (Foster et al., 1997).

Persistence of high values of ε_{TOC} through nearly 70 Ma of Gondwanan glaciation cannot, however, be ascribed simply to poor temporal resolution. Within the glaciation, the present record contains values of δ_o only for the 10-Ma increments centered on 255 ($n = 138$, Zechstein and North Sea), 265 ($n = 35$, North America and Bolivia), and 305 Ma ($n = 25$, North America and Germany). Mechanisms possibly underlying the persistence of large apparent differences between δ_a and δ_o are discussed near the end of this report, but the restricted coverage of these data shows clearly that further work is required.

3.1.3. Cretaceous and Cenozoic

Records for this time interval are shown in Fig. 3. Aspects of the timing of the isotopic variations, and ways in which they have interacted, are notable. First, although values of δ_a and δ_o vary significantly during this time interval, the net effect of those variations is to hold ε_{TOC} essentially constant at 30‰ until at least the middle Eocene. Second, the decline in carbon-isotopic fractionation, which has been recognized as characteristic of the Neogene (Arthur et al., 1985a; Popp et al., 1989; Kump and Arthur, 1997), actually begins in the Oligocene and proceeds at a nearly constant rate up to the Recent. Third, declines in δ_a together with increases in δ_o lead to an 8‰ change in ε_{TOC}, considerably larger than the change of roughly 5‰ that is observed in δ_o alone. Finally, changes in δ_a and ε_{TOC} combine to hold estimates of f_o essentially constant at approximately 0.25.

A principal uncertainty concerns the possibility of latitudinal effects. Marine organic matter forming at high latitudes today is significantly depleted in ^{13}C relative to that forming at temperate latitudes (e.g., Goericke and Fry, 1994). Accordingly, we must ask whether some artifacts of sampling, in which samples in older time intervals happen to be drawn preferentially from high paleolatitudes, is wholly or partly responsible for the observed isotopic shift. The likelihood of this can be judged crudely from Table 3, which shows no systematic poleward trend of paleolatitudes for older time intervals. Plots of δ_o as a function of paleolatitude for the Pleistocene, Pliocene, late Miocene, early Miocene, and late

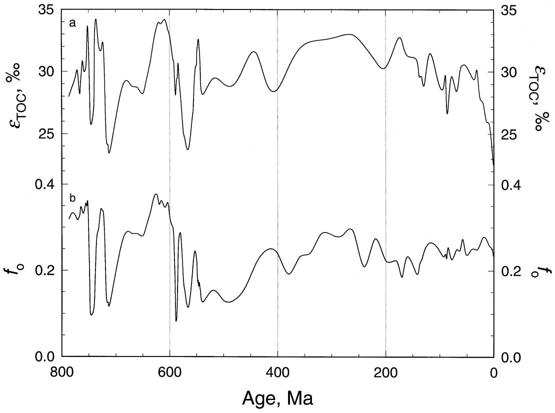

Fig. 4. The records of (a) carbon-isotopic fractionation and (b) f_o from Figs. 1–3, combined on a uniform time axis.

Oligocene (not shown here) are consistent with latitudinal gradients in δ_o, but the data are too sparse to allow estimation of the magnitude of those gradients. Indeed, there are no low-latitude points for the early Oligocene.

As a means of testing the sensitivity of these records to latitudinal effects, average values of δ_o for each time interval were recalculated after excluding all δ_o values with paleolatitudes equal to or greater than 45.0°. Results are indicated by the broken lines in Fig. 3b, c, and d. Significant changes in the computed-average value of δ_o occurred for the early Oligocene and for the early Eocene. In the former, the average value of δ_o was estimated to be equal to that in the late Oligocene, since δ_o values at high northern and southern latitudes appeared constant throughout the Oligocene. In the early Eocene, exclusion of relatively high δ_o values from sites 403 (49.1°N) and 338 (62.2°N) pulled the average down by 1.4‰. As can be seen by comparison of the records indicated by the broken- and unbroken-lines, such adjustments — if adopted — would alter the fine details but not the overall pattern of these isotopic variations.

3.2. Discussion of the records

The records assembled in Figs. 1–4 provide an answer to our first question, showing clearly that ε_{TOC} has varied significantly. These data are immediately useful for reconstruction of geochemical budgets. Secondarily, and in the remainder of this report, it is interesting to consider mechanisms possibly responsible for the observed variations in ε_{TOC}. The issue is not *exactly what* can be learned about ancient organisms or environmental conditions from these crude data but instead *what if anything* can be learned. How might these observations be understood, and in what ways do they fit existing ideas? Where do they not fit?

3.2.1. Factors controlling isotopic fractionation

As indicated schematically in Fig. 5, the isotopic difference denoted here by ε_{TOC} represents the combined effects of at least four natural processes: (i) the fractionation associated with fixation of CO_2 and production of biomass by primary producers, chiefly phytoplankton; (ii) the temperature-dependent fractionation between dissolved inorganic carbon (DIC) and dissolved CO_2, which is the substrate utilized by most primary producers, particularly at high concentrations (Raven, 1991); (iii) the fractionation between DIC and carbonate minerals; and (iv) whatever fractionations are associated with secondary biological processes ranging from grazing and heterotrophy in the water column through microbial reworking in sediments. Additionally, thermal processes can alter the ^{13}C content of sedimentary organic matter, mainly by preferentially mobilizing compounds that are depleted in ^{13}C relative to the bulk of the organic carbon. This process, however, becomes significant

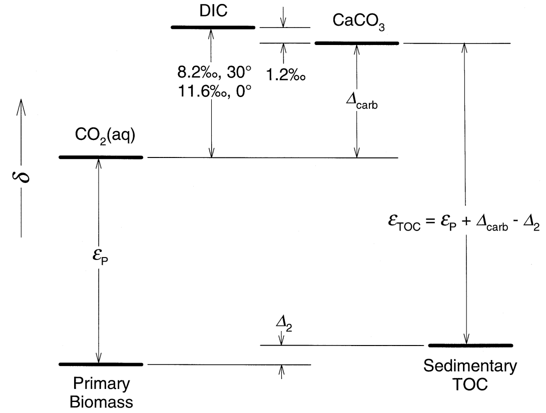

Fig. 5. Schematic summary of isotopic relationships between dissolved CO_2 and carbonate minerals, and between primary products and sedimentary TOC.

only as sediments are heated strongly enough to produce oil, a threshold that has been reached for few if any of the materials included here.

Following the definitions indicated graphically in Fig. 5, we can write:

$$\varepsilon_{\mathrm{TOC}} - \Delta_{\mathrm{carb}} = \varepsilon_{\mathrm{P}} - \Delta_2 , \tag{10}$$

where Δ_{carb} is the isotopic depletion of dissolved CO_2 in surface waters relative to sedimentary carbonates, ε_{P} is the isotope effect associated with primary production (Hayes et al., 1989, as modified by Freeman and Hayes, 1992) and Δ_2 is the isotopic shift associated with secondary biological processes (defined as positive when the residual organic matter is enriched in ^{13}C relative to primary biomass). As written, Eq. (10) places a measured parameter and a fractionation controlled mainly by chemical equilibria on its left side and leaves biological and environmental factors on its right. This arrangement points to a key problem: we can be relatively certain about the *net* isotopic fractionation imposed by biological processes, but, without more detailed information such as the isotopic compositions of primary biomarkers (e.g., Hayes et al., 1989), it is difficult to resolve the primary and secondary components of that fractionation.

Isotopic relationships between DIC, dissolved CO_2, and carbonate minerals have been reviewed by Freeman and Hayes (1992). Additional factors have recently been studied by Spero et al. (1997). As indicated in Fig. 5, Δ_{carb} has two components. The isotopic difference between dissolved CO_2 and DIC is large and quite strongly temperature dependent (0.12‰/C°). That between DIC and carbonate minerals is much smaller and only weakly temperature-dependent (0.01‰/C°). Its expression in natural settings can be explored by comparing the ^{13}C content of total sedimentary carbonate at 11 sites, worldwide (Shackleton, 1987) to the δ value of DIC in the overlying surface waters (Kroopnick, 1985). The average isotopic depletion in carbonate minerals relative to DIC, 1.2‰, is not correlated significantly either with latitude (44°N–43°S) or with surface water temperature (estimated annual average temperatures between 11° and 28°). In contrast, at equilibrium, dissolved CO_2 in seawater is depleted in ^{13}C relative to DIC by 8.2‰ at 30° and by 11.6‰ at 0°. As a result of the combination of these fractionations, Δ_{carb} is commonly 7‰ (= 8.2–1.2‰) where surface waters are warm and 10‰ where they are cold (the latter value being chosen on the assumption that calcareous sediments formed at sea-surface temperatures below 3° are not important components of the record). Boundary conditions for $\varepsilon_{\mathrm{P}} - \Delta_2$ can thus be defined using Eq. (10). Specifically, for temperatures between 3° and 30°:

$$\varepsilon_{\mathrm{TOC}} - 10 \le \varepsilon_{\mathrm{P}} - \Delta_2 \le \varepsilon_{\mathrm{TOC}} - 7. \tag{11}$$

The effects recently demonstrated by Spero et al. (1997) increase the 1.2‰ difference between DIC and carbonate minerals as concentrations of CO_3^{2-} increase. As a result, a greater portion of $\varepsilon_{\mathrm{TOC}}$ must be ascribed to $\varepsilon_{\mathrm{P}} - \Delta_2$, and the constants in Eq. (11) would be reduced. For $CaCO_3$, the effect amounts to 2‰ for a threefold increase in $[CO_3^{2-}]$ from present values.

Where secondary processes are dominated by respiratory remineralization, values of Δ_2 are expected to be small and positive (Hayes et al., 1989). This is borne out by observations in, e.g., the South Atlantic, where sedimentary TOC is enriched relative to planktonic organic carbon in the overlying water column by approximately 1.5‰ (Fischer et al., 1998). In the relatively short water column of the Santa Monica Basin, Gong and Hollander (1997) find $\Delta_2 \approx 0$ at the core top where bottom waters are oxic. In sediments underlying the upwelling zone in the Equatorial Pacific, Laarkamp and Raymo (1995) find that the flocculent organic material on the surface of the sediment is enriched in ^{13}C by about 0.5‰ relative to primary products (analyzed separately by Jasper et al., 1994) and that a further enrichment of as much as 3‰ takes place in the top 6 cm of the sediment as more than 80% of the organic carbon is remineralized. Such relatively large enrichments have also been observed in the Southern Ocean by Fischer (1991), but values of Δ_2 near 1.5‰ appear more generally representative of oxic conditions both there and at sediment depths greater than 100 cm in the Equatorial Pacific (Laarkamp and Raymo, 1995). Apparently, even under oxic conditions, Δ_2 responds to competing processes, with the balance of these commonly favoring enrichment on the order of 1.5‰.

Negative values of Δ_2, corresponding to depletion of ^{13}C in TOC relative to primary products, are observed when the range of processes includes secondary inputs from non-photosynthetic organisms. The best modern example is provided by the Black Sea, in which sulfide-oxidizing bacteria flourish in the water column. As is common in such settings, these chemoautotrophic organisms fix CO_2 at the oxycline, where DIC is depleted in ^{13}C relative to DIC in the photic zone. As a result, isotopically light organic carbon is added to the pool of TOC. Observations by Kodina et al. (1996) indicate that, at the same time that phytoplanktonic products averaged -22.5‰, values of δ_o for inputs from sulfide oxidizers were near -25.5‰. Examining sedimentary records, Arthur et al. (1994) found values of δ_o ranging from -22.1 to -26.0‰ and averaging -24‰, significantly depleted relative to phytoplanktonic products. Examining biologically controlled flows of carbon in the water column of the Black Sea, Karl and Knauer (1991) concluded that as much as 30% of the sinking particulate organic carbon could be derived from chemoautotrophic production. In the Santa Monica Basin, sediments accumulating at the depocenter are laminated because bottom waters there are poorly ventilated. At the periphery of the Basin, at water depths above the sill between the Basin and the open ocean, sediments are bioturbated and the boundary between aerobic and anaerobic conditions is not in the water column. Gong and Hollander (1997) have shown (i) that TOC in sediments at the depocenter is consistently depleted in ^{13}C relative to that in sediments on the periphery of the basin and (ii) via compound-specific analyses, that the depletion is associated with inputs from chemoautotrophs. Within the water column itself, production of isotopically depleted organic carbon, presumably by sulfide-oxidizing bacteria, is clearly evident at the depth of the sill, where aerobic and anaerobic waters are in contact (Hollander et al., unpublished observations).

Factors controlling ε_P have recently been discussed in very general terms, with agreement from theoretical considerations (Rau et al., 1997) and direct observations (Laws et al., 1997; Popp et al., 1998). An upper bound for ε_P is established by the isotope effect associated with carbon fixation. The expression of that isotope effect is attenuated as the growth rate increases, as the ratio of cellular volume to surface area increases, or as the concentration of dissolved CO_2 decreases. The magnitude of that attenuation is in turn dependent on the permeability of the algal cell wall. From observations of three representative species, Popp et al. (1998) found:

$$\varepsilon_P = 25.3 - 182(\mu/c_e)(V/S), \qquad (12)$$

where 25.3‰ is the isotope effect associated with fixation of carbon; the coefficient 182 is partly dependent on permeability; μ is the specific growth rate (/day); V/S is the cellular volume/surface area ratio (μm); and c_e is the concentration of dissolved CO_2 (μmol/kg). A plot of this relationship in terms of the concentration of dissolved CO_2, ε_P, and the rate of growth is shown in Fig. 6. The graph emphasizes a requirement imposed by the form of Eq. (12), namely that values of ε_P characteristic of phytoplankton (*modern* phytoplankton, at least) cannot exceed approximately 25‰. Considerably lower values will be observed where rates of growth are rapid or where concentrations of dissolved CO_2 are low. In the modern ocean, values of ε_P commonly range between 8 and 18‰ (e.g, Francois et al., 1993; Jasper et al., 1994; Bidigare et al., 1997).

3.2.2. Significance of variations in fractionation

Interactions between Δ_{carb}, ε_P, and Δ_2 are summarized graphically in Fig. 7. For any observed value of ε_{TOC}, it is necessary first to estimate the likely range of sea-surface temperatures, since that controls Δ_{carb} and, accordingly, provides boundary values for $\varepsilon_P - \Delta_2$ (see Eq. (10) and accompanying

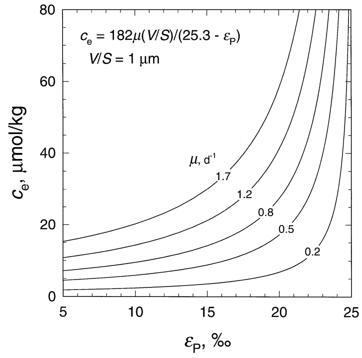

Fig. 6. Relationships between concentrations of dissolved CO_2 (c_e) and the isotopic fractionation associated with the production of primary biomass (ε_p) at representative rates of growth. Values of the coefficients in the equation are those reported by Popp et al. (1998).

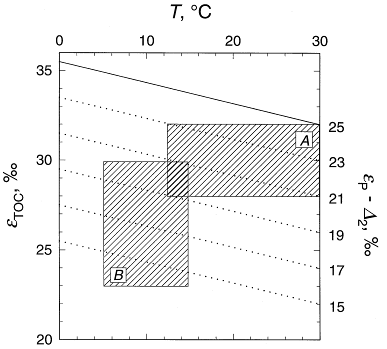

Fig. 7. Illustration of boundary–value relationships described in text, encompassing the range of values of ε_{TOC} encountered. T refers to the globally averaged temperature of productive ocean waters. The scale of values of $\varepsilon_P - \Delta_2$ shown at right pertains to the unbroken and dotted lines crossing the graph. The areas marked A and B are discussed in the text.

discussion). Given 25‰ as a maximum value for ε_P, observations falling above the unbroken line in Fig. 7 require $\Delta_2 \leq 0$ and are thus indicative of chemoautotrophic inputs. Other observations can be explained without requiring $\Delta_2 \leq 0$. Inputs from chemoautotrophs are not excluded in such cases — e.g., $\varepsilon_{TOC} = 30$‰ at $T \approx 10°$ might indicate $\varepsilon_P = 18.7$ and $\Delta_2 = -2.0$‰ — but the observation could be accounted for without calling for important levels of chemoautotrophy (i.e., by $20.7 \leq \varepsilon_P \leq 25$ and $0 \leq \Delta_2 \leq 4.3$). Increasing concentrations of CO_3^{2-} are expected to shift the lines on this graph downward.

Values of ε_{TOC} ranging between 28 and 32‰ (800–750 Ma and the Phanerozoic up to the Neogene, with possible exceptions in the Permo-Carboniferous and middle Jurassic) are generally associated with warm periods and would fall in region A in Fig. 7. These observations are generally consistent with oxic reworking of phytoplanktonic products, given some combination of slower rates of growth, higher levels of CO_2, and smaller V/S ratios.

Estimated values of ε_{TOC} exceed 32‰ at four intervals during the Cambrian–Jurassic time span. Of these, two occurrences have statistical significance. One, from the middle Jurassic, represents only two analyses of shales from the Tarim Basin, China (the trend lines in Fig. 2 ignore this point), and the other, from the middle Permian, is controlled entirely by samples from the Phosphoria Formation. If representative of a strong zone of upwelling, the latter depositional environment may well not have been globally representative. Additionally, DIC available in surface waters in these paleoenvironments may have been depleted in ^{13}C relative to the open-ocean settings represented by the δ_a record. Given the relative prominence of continental and near-shore sediments among samples not collected from ocean-drilling cores, this factor may have subtly but broadly influenced the pre-Cretaceous record of δ_o.

Marked occurrences of $\varepsilon_{TOC} > 32$‰ are observed in the Neoproterozoic at 610–620 Ma, just prior to the Varanger ice ages, and at 740 and 760 Ma, in between and just prior to the two Sturtian ice ages. Examination of the databases shows that these values have not been shifted upward by inclusion of isotopically enriched dolomites in the records of δ_a. Notably, Canfield and Teske (1996) have interpreted the sulfur-isotopic record and molecular–biologic evidence as indicating that sulfide-oxidizing bacteria radiated and flourished during these intervals. More recently, Canfield (1998) has shown that deep ocean waters were probably anaerobic and sulfidic until late in the Proterozoic. The oxygenation of surface environments that made the Cambrian explosion possible also drove the oxygenation of the deep ocean, and levels of O_2 must have been held down until that redox buffer was saturated. The oxidation of deep-sea sulfide would have been microbially catalyzed and considerable amounts of chemosynthetic bacterial biomass thus produced. Incorporation of these products in sediments would push Δ_2 to negative values. In short, the carbon isotopic evidence is consistent with the independent inferences based on sulfur-isotopic and molecular–biologic evidence.

Values of ε_{TOC} ranging down to 23‰ (region B, Fig. 7) are associated with some, but not all, of the cooler periods of earth history, specifically the Sturtian (740, 720 Ma) and Varangerian (590, 575 Ma) glaciations and the Neogene cooling. Notably, estimated values of f_o (Fig. 4b) vary only slightly during the Neogene, but strongly during the Neoproterozoic. The earlier events have been described as yielding a ''Snowball Earth'' (Kirschvink, 1992; Hoffman et al., 1998) in which ice margins normally found at polar latitudes met at the equator, entombing the planet in pack ice and continental glaciers and halting the hydrologic cycle. The present ice age is, clearly, less severe, but solar luminosity is now 6–7% higher than during the Neoproterozoic (Gough, 1981; Kasting, 1992). The rough equality between Neoproterozoic and Pleistocene values of ε_{TOC} is plausibly indicative of similar concentrations of CO_2 in productive ocean waters which, given the different solar luminosities, may have yielded a global snowball during the Neoproterozoic and icecaps during the Pleistocene. Alternative or additional factors would include high V/S ratios or rapid rates of growth. Mendelson and Schopf (1992) have summarized occurrences of particularly large acritarchs throughout the Neoproterozoic. If these organisms were phytoplanktonic and dominant in producer communities, such organisms might have yielded particularly low values of ε_P. The paleontological record does not indicate that their abundance peaked during the low-ε_{TOC} episodes, but they did die out during the terminal Proterozoic and lower Cambrian. High rates of oceanic circulation, driven by strong temperature gradients during icehouse episodes, might also have fertilized surface waters and sustained rapid rates of algal growth.

The Neoproterozoic records available at present are interesting rather than definitive. The low-ε features all include cases in which both organic carbon and carbonate carbon have been analyzed in the same sample. But the *durations* of these features are influenced strongly by comparisons of δ_o and δ_a values from different basins. Revised stratigraphic correlations could thus pinch these features strongly. Moreover, estimates of the abundances and fluxes of carbon (Hoffman et al., 1998) suggest extraordinary fluctuations during glacial advances and retreats. The dramatic variations in the isotopic records are well-matched with the dramatic climatic and environmental variations, but no systematic interpretation can yet be offered.

Values of ε_{TOC} observed since the Eocene also fall in region B of Fig. 7, and this record can be considered in more detail. Representative values of ε_{TOC} and their likely relationships to ε_P are summarized graphically in Fig. 8. In this sequence, it is postulated that globally averaged values of Δ_{carb} increased from 7.5 to 8.5‰ as surface temperatures declined, and that conditions of ocean ventilation at sites sampled by the ocean drilling programs were such that Δ_2 remained constant at 1.5‰. In those circumstances, average values of ε_P would have declined as shown from roughly 24 to 15.4‰. No significant carbonate effect is postulated. If concentrations of CO_3^{2-} increased strongly, values of Δ_{carb} would be decreased and estimated values of ε_P increased. For reference, the Pleistocene relationships depicted in Fig. 8 would correspond to sedimentary $\delta_a = +0.2$‰, $\delta_{CO2} = -8.3$‰, primary products with $\delta = -23.3$‰, and sedimentary $\delta_o = -21.8$‰.

The changing values of ε_P must reflect changes in one or more of the parameters in Eq. (12). The graph shown in Fig. 9 provides a means of considering such variations. In it, concentrations of dissolved CO_2 (c_e) and specific growth rates (μ) are expressed relative to those characteristic of the Pleistocene. The lines represent $c_e - \varepsilon_P$ relationships, at the indicated relative rates of growth, for phytoplanktonic communities with V/S ratios equal to that prevailing during the Pleistocene. The reference point indicative of Pleistocene conditions is shown at lower left, at $\varepsilon_P = 15.4$‰ and relative $c_e = 1$. Points representative of the other times shown in Fig. 8 are plotted at the corresponding values of ε_P. For example, the value of ε_P estimated for the late Oligocene (21.9‰, see Fig. 8), would correspond to relative $c_e = 2.9$ if the average rate of growth were equal to that during the Pleistocene, or to relative $c_e = 1.4$ if, presumably due to slower delivery of nutrients to surface water, average rates of growth during the late Oligocene were half as rapid as those during the Pleistocene.

The Oligocene-to-Pleistocene decrease in ε_P could also be ascribed in part to a systematic increase in globally averaged V/S ratios over this same time span. To whatever extent this occurred, the c_e axis in Fig. 9 would be compressed, with estimated concentrations of CO_2 during the Oligocene exceeding Pleistocene values by a smaller factor. There is organic geochemical evidence for a trend of this kind, since relative concentrations of C_{28} steranes, for which diatoms are a prominent source, increase significantly over this time interval (Grantham and Wakefield, 1988). An even larger increase in the relative abundance of C_{28} steranes, however, precedes the Cenozoic, let alone the Neogene. To further examine the importance of large

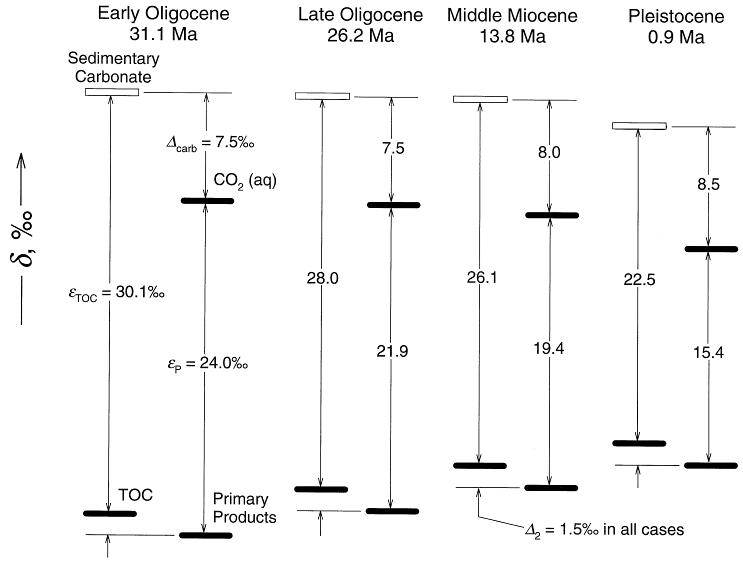

Fig. 8. Graphical summary of varying isotopic relationships probably underlying the observed decrease in values of ε_{TOC}, early Oligocene to Pleistocene.

diatoms as shapers of the isotopic record, we have computed separate records of δ_o for sediments from the Atlantic (minimal inputs from diatoms) and Pacific and Southern Oceans (relatively abundant diatoms). These show that δ_o has increased in both regions, with the average difference between them not differing significantly from zero. Accordingly, if a V/S trend is partly responsible for the decline in ε_P, that trend is probably *not* being driven by diatoms.

The uncertainties highlighted by these considerations of Figs. 8 and 9 are reminders of the advantages of more tightly focused proxies. Compound-specific isotopic analyses of primary products can eliminate concerns about the unknown magnitude of Δ_2 and, if the range of producers is narrow enough, about changes in V/S. Even so, it will be necessary to resolve effects of c_e and μ, and to deal with relationships between measurable values of δ_a and the isotopic composition of dissolved CO_2.

Finally, we can return to the question of maximal values for ε_P. The 25.3‰ maximum indicated by Eq. (12) derives from studies of only a few species. Its significance can, however, be strongly buttressed. First, there are no reports of phytoplanktonic products in nature or in laboratory studies for which the isotopic compositions require $\varepsilon_P > 25$‰. Second, the 28–32‰ plateau for values of ε_{TOC}, which is representative of most of the Phanerozoic and significant portions of the Neoproterozoic, can be straightforwardly interpreted as a manifestation of a 25‰-maximum value for ε_P. Third, the values of ε_{TOC} greater than 32‰ that occur prominently during the Neoproterozoic, and which could be representative

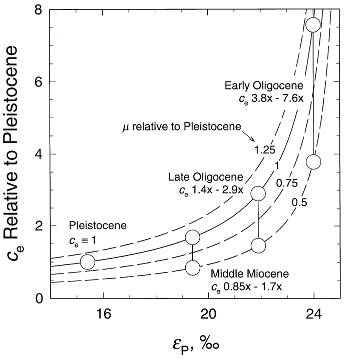

Fig. 9. Possible relationships between concentrations of dissolved CO_2, isotopic fractionation, and rate of growth for a phytoplanktonic community with an average (volume/surface area) ratio like that of the Pleistocene. Concentrations of dissolved CO_2 (c_e) and rates of growth (μ) are expressed relative to Pleistocene values. The values of ε_P are those estimated in Fig. 8.

of $\varepsilon_P > 25‰$, are more satisfactorily interpreted in terms of chemoautotrophic inputs, for which there is independent evidence. Fourth, interpretation of any part of the record as representative of $\varepsilon_P > 25‰$ would require, on present biological evidence, simultaneous acceptance of the idea that a super-fractionating mechanism of carbon fixation, once globally dominant, had since disappeared without a trace. On balance, we consider that acceptance of 25‰ as a maximum value for globally representative values of ε_P is a strong working hypothesis.

3.2.3. The exogenic cycle and burial of carbon

The record of f_o shown in Fig. 4 is a crude estimate based on the assumption that the isotopic composition of carbon entering the exogenic cycle has remained constant at −5‰ vs. PDB. Its values are, therefore, not equivalent to those of X_{org}^{bur}, the organic-carbon-burial mole fraction defined by Derry and France-Lanord (1996), which takes explicit account of variations in the isotopic composition of recycling carbon. Still less do they specify net burial fluxes of organic carbon, which can be determined only after rates of erosion have been estimated (Derry and France-Lanord, 1996). With those caveats, however, several features of the curve displayed in Fig. 4 may point to subjects for further study. Since the early Devonian, the net effect of variations in δ_a and ε_{TOC} has been to constrain variations in f_o, holding it near 0.25. Indeed, estimated variations in f_o diminish as the available records of δ_a and δ_o improve (i.e., for times covered by cores of oceanic sediments). Does this reflect the operation of feedback-control mechanisms which stabilized pO_2? At earlier times — notably, prior to the development of extensive and substantial populations of plants on land — variations in f_o appear to have been much larger. As noted earlier (Knoll et al., 1986; Derry et al., 1992), intervals in the Neoproterozoic were characterized by high values of f_o that may well have been related to a global rise in atmospheric pO_2 and the subsequent development of animals with relatively high demands for O_2. Additionally, the Sturtian (740, 720 Ma) and Varangerian (590, 575 Ma) glaciations are all marked by precipitous drops in estimated values of f_o. These suggest a marked preference for deposition of carbonates rather than organic carbon and may be related to the formation of the ''cap carbonates'' (Fairchild, 1993) which are so prominent in these successions. As a result of variations in δ_a and δ_o, this signal appears strongly for the first Varanger glaciation even though variations in ε_{TOC} are small relative to those observed during the other Neoproterozoic glaciations (compare Fig. 4a and b at 590 Ma).

3.2.4. Comparisons to alternative estimates

Geochemical models, isotopic analyses of pedogenic carbonates in paleosols, and stomatal indices (all reviewed by Berner, 1997) concordantly indicate a return to near-present concentrations of CO_2 in the atmosphere and oceans at the time of the Gondwanan glaciations, 250–320 Ma ago. If this concordance is accepted as definitive, we are left to search for explanations for the constancy, and high values, of ε_{TOC} through this same interval. Two sets of factors can be identified. In their diversity and marginal plausibility, they point to a need for many more, and more highly specific, isotopic analyses of sedimentary organic carbon during the Gondwanan glaciation and, indeed, throughout the Paleozoic.

3.2.4.1. Depositional. The record is very sparse and biased towards epicratonic sediments that, in spite of attempts to avoid terrigenous influences, may have been particularly susceptible to them. Perhaps sequestration of nutrients by land plants was so strong that marine productivity was diminished. Terrigenous inputs, both aeolian and riverine, thus gained in importance and may have been enriched in lipids and lignin-related components, both so strongly depleted in ^{13}C relative to whole-plant carbon that values of δ_o were driven down even though Permian and Carboniferous coals are enriched in ^{13}C relative to coeval marine sediments. The same effects would not have been observed during the Neoproterozoic glaciations because land plants were absent.

3.2.4.2. Biological and environmental. As permitted by the uncertainties in the alternative lines of evidence (paleosols, etc.), concentrations of CO_2 might actually have declined only to levels about threefold greater than those at present. Values of ε_P could then have been as high as 23.5‰ if the average V/S ratio were half that at present (and/or permeabilities of algal cell walls were higher). For cold surface waters, values of ε_{TOC} as high as 32‰ could thus be accommodated. In other words, the excursion to low levels of CO_2 during the glaciation may have been very poorly recorded because ε_{TOC} was so near its maximum values.

Possible carbonate effects (Spero et al., 1997) do not help to explain the absence of isotopic signals because they tend to increase estimated values of ε_P. And it is not attractive to call for high inputs from chemoautotrophs (and thus $\Delta_2 < 0$, which would yield lower estimates of ε_P) during a glacial interval, since strong temperature gradients are expected to invigorate circulation and prevent development of anaerobic bottom waters.

For the Cenozoic, mass-balance models and paleosol data (Berner, 1994, 1997) indicate CO_2 levels only slightly lower than those indicated in Fig. 9. The discordance could be neutralized by changes in V/S or in cell-wall permeability.

4. Conclusions

The records of ε_{TOC} developed here are consistent with the occurrence of Pleistocene levels of CO_2 during the Neoproterozoic glaciations (Kasting, 1992). The high values of ε_{TOC} observed during non-glaciated intervals of the Neoproterozoic suggest globally significant accumulation of chemoautotrophic products in oceanic sediments, and thus provide support for suggestions that the deeper waters of Proterozoic oceans were sulfidic (Canfield, 1998), and that sulfide-oxidizing bacteria flourished and developed during these time intervals (Canfield and Teske, 1996).

The estimates of f_o compiled here suggest that the (organic carbon burial/total carbon burial) ratio has probably varied by less than 25% since the Devonian and by less than 10% since the early Oligocene. By contrast, there is good evidence that the same ratio varied widely during the Neoproterozoic, quite possibly over a fourfold range.

The structure of the record of ε_{TOC} strongly suggests that the maximum isotopic fractionation associated with photosynthetic fixation of carbon being unchanged for 800 Ma.

There is compelling evidence that values of ε_{TOC} have varied widely, at least between 23 and 34‰, and that the long-term average is roughly 30‰ rather than the value of 25‰ frequently employed in carbon-cycle models. In particular, there is compelling evidence for wide, climatically linked variations of ε_P during the Neoproterozoic, with minima being closely associated with glaciations. Finally, there is very strong evidence that globally averaged values of ε_{TOC} have declined almost linearly since the early Oligocene.

Acknowledgements

We thank Jan Veizer for his dedicated leadership of the Earth Systems Evolution program of the Canadian Institute for Advanced Research (CIAR). It is from the work and discussions of that group that this paper has developed. We thank U. Berner, BGR-Hannover, Germany, for providing an unpublished, organic-carbon isotopic dataset. We thank David Rowley, University of Chicago, for calculation of paleolatitudes of Cretaceous and Cenozoic samples. HS notes that this article is a contribution to IGCP project No. 386. J.M.H. thanks NASA (NAG5-6660) and the CIAR for support and notes that this is Woods Hole Oceanographic Institution contribution no. 9947. We are grateful for excellent formal reviews of this manuscript by Thure Cerling, Michael Lewan, and Brian Popp, and for very helpful comments from Bob Berner, Gerhard Fischer, Galen Halvorson, Andy Knoll, Lee Kump, Graham Logan, Greg Rau, and Roger Summons.

References

Arthur, M.A., Dean, W.E., Claypool, G.E., 1985a. Anomalous ^{13}C enrichment in modern marine organic carbon. Nature 295, 216–218.

Arthur, M.A., Dean, W.E., Schlanger, S.O., 1985b. Variations in the global carbon cycle during the Cretaceous related to climate, volcanism and changes in atmospheric CO_2. In: Sundquist, E.T., Broecker, W.S. (Eds.), The Carbon Cycle and Atmospheric CO_2: Natural Variations Archean to Present, Geophysical Monograph 32, American Geophysical Union, Washington, pp. 504–529.

Arthur, M.A., Dean, W.E., Neff, E.D., Hay, B.J., King, J., Jones, G., 1994. Varve-calibrated records of carbonate and organic carbon accumulation over the last 2000 years in the Black Sea. Global Biogeochemical Cycles 8, 195–217.

Asmerom, Y., Jacobsen, S.B., Knoll, A.H., Butterfield, N.J., Swett, K., 1991. Strontium isotopic variations of Neoproterozoic seawater: implications for crustal evolution. Geochim. Cosmochim. Acta 55, 2883–2894.

Bartley, J.K., Pope, M., Knoll, A.H., Semikhatov, M.A., Kolosov, P.Yu., 1998. A Vendian–Cambrian boundary succession from the northwestern margin of the Siberian Platform: stratigraphy, palaeontology, chemostratigraphy and correlation. Geological Magazine 135, 473–494.

Berggren, W.A., Kent, D.V., Swisher III, C.C., Aubry, M.-P., 1995. A revised Cenozoic geochronology and chronostratigraphy. In: Geochronology Time Scales and Global Stratigraphic Correlation. SEPM Special Publication No. 54, SEPM (Society for Sedimentary Geology), pp. 129–212.

Berner, R.A., 1994. Geocarb II: a revised model of atmospheric CO_2 over Phanerozoic time. Am. J. Sci. 294, 56–91.

Berner, R.A., 1997. The rise of plants and their effect on weathering and atmospheric CO_2. Science 276, 544–546.

Bertrand-Sarfati, J., Moussine-Pouchkine, A., Amard, B., Ait-Kaci, A., 1995. First Ediacaran fauna found in western Africa and evidence for an Early Cambrian glaciation. Geology 23, 133–136.

Bidigare, R.R., Fluegge, A., Freeman, K.H., Hanson, K.L., Hayes, J.M., Hollander, D., Jasper, J.P., King, L.L., Laws, E.A., Milder, J., Millero, F.J., Pancost, R., Popp, B.N., Sternberg, P.A., Wakeham, S.G., 1997. Consistent fractionation of ^{13}C in nature and in the laboratory: growth-rate effects in some haptophyte algae. Global Biogeochemical Cycles 11, 279–292.

Bowring, S.A., Grotzinger, J.P., Isachsen, C.E., Knoll, A.H., Pelechaty, S.M., Kolosov, P., 1993. Calibrating rates of Early Cambrian evolution. Science 261, 1293–1298.

Buchardt, B., Holmes, M.A., 1995. Initial transgressive phase of Leg 144 guyots: evidence of extreme sulfate reduction. In: Haggerty, J.A., Premoli Silva, A., Rack, F., McNutt, M.K. (Eds.), Proc. ODP, Sci. Results, 144. Ocean Drilling Program, College Station, TX, pp. 895–913.

Calder, J.A., Horvath, G.J., Shultz, D.J., Newman, J.W., 1974. Geochemistry of the stable carbon isotopes in some Indian Ocean sediments. In: Davies, T.A., Luyendyk, B.P., et al. (Eds.), Init. Rep. DSDP, 26. U.S. Govt. Printing Office, WA, pp. 613–617.

Canfield, D.E., 1998. A new model for Proterozoic ocean chemistry. Nature (in press).

Canfield, D.E., Teske, A., 1996. Late Proterozoic rise in atmospheric oxygen concentration inferred from phylogenetic and sulphur-isotope studies. Nature 382, 127–132.

Dean, W.E., 1981. Calcium carbonate and organic carbon in samples from Deep Sea Drilling Project sites 463, 464, 465, and 466. In: Thiede, J., Vallier, T.L., et al. (Eds.), Init. Rep. DSDP, 62. U.S. Govt. Printing Office, WA, pp. 869–890.

Dean, W.E., Arthur, M.A., 1987. Inorganic and organic geochemistry of Eocene to Cretaceous strata recovered from the lower continental rise, North American Basin, site 603, Deep Sea Drilling Project Leg 93. In: van Hinte, J.E., Wise, S.W., et al. (Eds.), Init. Rep. DSDP, 93. U.S. Govt. Printing Office, WA, pp. 1093–1137.

Degens, E.T., 1969. Biogeochemistry of stable carbon isotopes. In: Eglinton, G., Murphy, M.T.J. (Eds.), Organic Geochemistry. Springer-Verlag, New York, pp. 304–329.

Derry, L.A., France-Lanord, C., 1996. Neogene growth of the sedimentary organic carbon reservoir. Paleoceanography 11, 267–275.

Derry, L.A., Kaufman, A.J., Jacobsen, S.B., 1992. Sedimentary cycling and environmental change in the Late Proterozoic: evidence from stable and radiogenic isotopes. Geochim. Cosmochim. Acta 56, 1317–1329.

Dunham, K.W., Meyers, P.A., Ho, E.S., 1988. Organic geochemistry of Cretaceous black shales and adjacent strata from the Galicia Margin, North Atlantic Ocean. In: Boillot, G., Winterer, E.L., et al. (Eds.), Proc. ODP, Sci. Results, 103. Ocean Drilling Program, College Station, TX, pp. 557–565.

Erdman, J.G., Schorno, K.S., 1978. Geochemistry of carbon: Deep Sea Drilling Project leg 38. In: Talwani, M., Udintsev, G., et al. (Eds.), Init. Rep. DSDP, 38. U.S. Govt. Printing Office, WA, pp. 791–799.

Erdman, J.G., Schorno, K.S., 1978. Geochemistry of carbon: Deep Sea Drilling Project leg 40. In: Bolli, H.M., Ryan, W.B.F., et al. (Eds.), Init. Rep. DSDP, 40 (Suppl.). U.S. Govt. Printing Office, WA, pp. 651–658.

Erdman, J.G., Schorno, K.S., 1978. Geochemistry of carbon: Deep Sea Drilling Project leg 41. In: Lancelot, Y., Seibold, E., et al. (Eds.), Init. Rep. DSDP, 41. U.S. Govt. Printing Office, WA, pp. 849–853.

Erdman, J.G., Schorno, K.S., 1978. Geochemistry of carbon: Deep Sea Drilling Project leg 44. In: Benson, W.E., Sheridan, R.E., et al. (Eds.), Init. Rep. DSDP, 44. U.S. Govt. Printing Office, WA, pp. 605–615.

Erdman, J.G., Schorno, K.S., 1979. Geochemistry of carbon: Deep Sea Drilling Project legs 47A and B. In: Sibuet, J.-C., Ryan, W.B.F., et al. (Eds.), Init. Rep. DSDP, 47, Part 2. U.S. Govt. Printing Office, WA, pp. 553–559.

Erdman, J.G., Schorno, K.S., 1979. Geochemistry of carbon: Deep Sea Drilling Project leg 48. In: Montadert, L., Roberts, D.G., et al. (Eds.), Init. Rep. DSDP, 48. U.S. Govt. Printing Office, WA, pp. 947–950.

Fairchild, I.J., 1993. Balmy shores and icy wastes: the paradox of carbonates associated with glacial deposits in Neoproterozoic times. In: Wright, V.P. (Ed.), Sedimentology Review 1, Blackwell, Oxford, UK, pp. 1–16.

Fairchild, I.J., Spiro, B., 1987. Petrological and isotopic implications of some contrasting Late Precambrian carbonates, NE Spitsbergen. Sedimentology 34, 973–989.

Fischer, G., 1991. Stable carbon isotope ratios of plankton carbon and sinking organic matter from the Atlantic sector of the Southern Ocean. Mar. Chem. 35, 581–596.

Fischer, G., Müller, P.J., Wefer, G., 1998. Latitudinal $\delta^{13}C_{org}$ variations in sinking matter and sediments from the South Atlantic: effects of anthropogenic CO_2 and implications for palaeo-PCO_2 reconstructions. J. Mar. Sci. (in press).

Foster, C.B., Logan, G.A., Summons, R.E., Gorter, J.D., Edwards, D.S., 1997. Carbon isotopes, kerogen types and the Permian–Triassic boundary in Australia: implications for exploration. APPEA Journal 1997, 472–489.

Francois, R., Altabet, M.A., Goericke, R., McCorkle, D.C., Brunet, C., Poisson, A., 1993. Changes in the δ^{13}C of surface water particulate organic matter across the subtropical convergence in the SW Indian Ocean. Global Biogeochemical Cycles 7, 627–644.

Freeman, K.H., Hayes, J.M., 1992. Fractionation of carbon isotopes by phytoplankton and estimates of ancient CO_2 levels. Global Biogeochemical Cycles 6, 185–198.

Galimov, E.M., Kodina, L.A., Shirinsky, V.G., Drozdova, T.V., Generalova, V.N., Bogacheva, M.P., Chinyonov, V.A., Bannikova V.I., 1980. A study of organic matter from deep ocean bore holes, Deep Sea Drilling Project sites 415 and 416, in the Moroccan Basin. In: Lancelot, Y., Winterer, E.L., et al. (Eds.), Init. Rep. DSDP, 50. U.S. Govt. Printing Office, WA, pp. 575–603.

Goericke, R., Fry, B., 1994. Variations of marine plankton δ^{13}C with latitude, temperature, and dissolved CO_2 in the world ocean. Global Biogeochemical Cycles 8, 85–90.

Gong, C., Hollander, D.J., 1997. Differential contribution of bacteria to sedimentary organic matter in oxic and anoxic environments, Santa Monica Basin, California. Org. Geochem. 26, 545–563.

Gough, D.O., 1981. Solar interior structure and luminosity variations. Solar Physics 74, 21–34.

Grantham, P.J., Wakefield, L.L., 1988. Variations in the sterane carbon number distributions of marine source rock derived crude oils through geological time. Org. Geochem. 12, 61–73.

Grotzinger, J.P., Bowring, S.A., Saylor, B.Z., Kaufman, A.J., 1995. Biostratigraphic and geochronologic constraints on early animal evolution. Science 270, 598–604.

Harland, W.B., Armstrong, R.L., Cox, A.V., Craig, L.E., Smith, A.G., Smith, D.G., 1990. A Geologic Time Scale 1989. Cambridge Univ. Press, Cambridge, UK.

Hayes, J.M., 1983. Geochemical evidence bearing on the origin of aerobiosis, a speculative interpretation. In: Schopf, J.W. (Ed.), The Earth's Earliest Biosphere: Its Origin and Evolution. Princeton University Press, Princeton, NJ, pp. 291–301.

Hayes, J.M., Kaplan, I.R., Wedeking, K.W., 1983. Precambrian organic geochemistry, preservation of the record. In: Schopf, J.W. (Ed.), The Earth's Earliest Biosphere: Its Origin and Evolution. Princeton University Press, Princeton, NJ, pp. 93–134.

Hayes, J.M., Popp, B.N., Takigiku, R., Johnson, M.W., 1989. An isotopic study of biogeochemical relationships between carbonates and organic carbon in the Greenhorn Formation. Geochim. Cosmochim. Acta 53, 2961–2972.

Heaman, L.M., Rainbird, R.H., 1990. A U-Pb baddelyite study of Franklin igneous events, Canada. Geol. Assoc. Canada Miner. Assoc. Canada Prog. 15, p. A55.

Hoffman, P.F., Hawkins, D.P., Isachsen, C.E., Bowring, S.A., 1996. Precise U-Pb zircon ages for early Damaran magmatism in the Summas Mountains and Welwitschia Inlier, northern Damara belt, Namibia. Geological Survey of Namibia Communications 11, 47–52.

Hoffman, P.F., Kaufman, A.J., Halverson, G.P., Schrag, D.P., 1998. A Neoproterozoic snowball earth. Science 281, 1342–1346.

Hoffman, P.F., Kaufman, A.J., Halverson, G.P., in press. Comings and goings of global glaciations on a Neoproterozoic tropical platform in Namibia. GSA Today.

Holser, W.T., Schidlowski, M., Mackenzie, F.T., Maynard, J.B., 1988. Geochemical cycles of carbon and sulfur. In: Gregor, C.B., Garrels, R.M., Mackenzie, F.T., Maynard, J.B. (Eds.), Chemical Cycles in the Evolution of the Earth. Wiley, New York, pp. 105–173.

Jasper, J.P., Hayes, J.M., Mix, A.C., Prahl, F.G., 1994. Photosynthetic fractionation of ^{13}C and concentrations of dissolved CO_2 in the central equatorial Pacific during the last 255,000 years. Paleoceanography 9, 781–798.

Karl, D.M., Knauer, G.A., 1991. Microbial production and particle flux in the upper 350 m of the Black Sea. Deep-Sea Res. 38 (2), S921–S942, Suppl.

Kasting, J.F., 1992. Proterozoic climates: the effect of changing atmospheric carbon dioxide concentrations. In: Schopf J.W., Klein, C. (Eds.), The Proterozoic Biosphere, A Multidisciplinary Study. Cambridge Univ. Press, Cambridge, UK, pp. 165–168.

Katz, B.J., 1988. Organic–geochemical character and hydrocarbon-source potential of site 635. In: Austin, Jr. J.A., Schlager, W. et al., Proc. ODP, Sci. Results, 101. Ocean Drilling Program, College Station, TX, pp. 381–388.

Kaufman, A.J., Knoll, A.H., 1995. Neoproterozoic variations in the carbon isotopic composition of seawater: stratigraphic and biogeochemical implications. Precambrian Research 73, 27–49.

Kaufman, A.J., Hayes, J.M., Knoll, A.H., Germs, G.J.B., 1991. Isotopic compositions of carbonates and organic carbon from Upper Proterozoic successions in Namibia: stratigraphic variation and the effects of diagenesis and metamorphism. Precambrian Research 49, 301–327.

Kaufman, A.J., Knoll, A.H., Semikhatov, M.A., Grotzinger, J.P., Jacobsen, S.B., Adams, W.R., 1996. Isotopic chemostratigraphy of Precambrian–Cambrian boundary beds in the Western Anabar Region, Northern Siberia. Geol. Mag. 133, 509–533.

Kaufman, A.J., Knoll, A.H., Narbonne, G.M., 1997. Isotopes, ice ages, and terminal Proterozoic earth history. Proceedings of the National Academy of Sciences 94, 6600–6605.

Kennicutt II, M.C., Brooks, J.M., McDonald, T.J., Pflaum, R.C., 1985. Nonvolatile organic matter at sites 565–570, Deep Sea Drilling Project Leg 84. In: von Huene, R., Aubouin, J., et al., Init. Rep. DSDP, 84. U.S. Govt. Printing Office, WA, pp. 705–717.

Kimura, H., Matsumoto, R., Kakuwa, Y., Hamdi, B., Zibaseresht, H., 1997. The Vendian–Cambrian δ^{13}C record, North Iran: evidence for overturning of the ocean before the Cambrian explosion. Earth Planet. Sci. Lett. 147, E1–E7.

Kirschvink, J.L., 1992. Late Proterozoic low-latitude global glaciation: the snowball earth. In: Schopf, J.W., Klein, C. (Eds.), The Proterozoic Biosphere, a Multidisciplinary Study. Cambridge Univ. Press, Cambridge, UK, pp. 51–52.

Knoll, A.H., Hayes, J.M., Kaufman, A.J., Swett, K., Lambert, I.B., 1986. Secular variations in carbon isotope ratios from Upper Proterozoic successions of Svalbard and East Greenland. Nature 321, 832–838.

Knoll, A.H., Grotzinger, J.P., Kaufman, A.J., Kolosov, P., 1995a.

Integrated chronostratigraphy of the terminal Proterozoic successions of the Olenek Uplift, northern Siberia. Precambrian Research 73, 251–270.

Knoll, A.H., Kaufman, A.J., Semikhatov, M.A., Grotzinger, J.P., Adams, W.R., 1995b. Sizing up the sub-Tommotian unconformity in Siberia. Geology 23, 1139–1143.

Kodina, L.A., Bogacheva, M.P., Lyutsarev, S.B., 1996. Particulate organic carbon in the Black Sea: isotopic composition and origin. Geochemistry International 34, 798–804, Geokhimiya (1996) 884–890.

Kroopnick, P., 1985. The distribution of ^{13}C in ΣCO_2 in the world oceans. Deep-Sea Res. 32, 57–84.

Kump, L.R., 1989. Alternative modeling approaches to the geochemical cycles of carbon, sulfur, and strontium isotopes. Am. J. Sci. 289, 390–410.

Kump, L.R., Arthur, M.A., 1997. Global chemical erosion during the Cenozoic: weatherability balances the budgets. In: Ruddiman, W.F. (Ed.), Tectonic Uplift and Climate Change. Plenum, New York, pp. 399–426.

Laarkamp, K.L., Raymo, M.E., 1995. Carbon isotopic composition of particulate organic material from the interior of the Equatorial Pacific Ocean. ICP V Program and Abstracts, 5th International Conference on Paleoceanography. University of New Brunswick, Fredricton, p. 132.

Laws, E.A., Bidigare, R.R., Popp, B.N., 1997. Effect of growth rate and CO_2 concentration on carbon isotopic fractionation by the marine diatom *Phaeodactylum tricornutum*. Limnol. Oceanogr. 42, 1152–1560.

Lewan, M.D., 1986. Stable carbon isotopes of amorphous kerogen from Phanerozoic sedimentary rocks. Geochim. Cosmochim. Acta 50, 1583–1591.

Macko, S.A., 1989. Stable isotope organic geochemistry of sediments from the Labrador Sea (Sites 646 and 647) and Baffin Bay (Site 645), ODP Leg 105. In: Srivastava, S.P., Arthur, M., Clement, B. et al., (Eds.), Proc. ODP, Sci. Results, 105. Ocean Drilling Program, College Station, TX, pp. 209–231.

Macko, S.A., Pereira, C.P.G., 1990. Neogene paleoclimate development of the Antarctic Weddell Sea region: organic geochemistry. In: Barker, P.F., Kennett, J.P., et al. (Eds.), Proc. ODP, Sci. Results, 113. Ocean Drilling Program, College Station, TX, pp. 881–897.

Mendelson, C.V., Schopf, J.W., 1992. Proterozoic and Early Cambrian acritarchs. In: Schopf, J.W., Klein, C. (Eds.), The Proterozoic Biosphere, a Multidisciplinary Study. Cambridge Univ. Press, Cambridge, UK, pp. 219–232.

Muzuka, A.N.N., Macko, S.A., Pedersen, T.F., 1991. Stable carbon and nitrogen isotope compositions of organic matter from sites 724 and 725, Oman Margin. In: Prell, W.L., Niitsuma, N., et al. (Eds.), Proc. ODP, Sci. Results, 117. Ocean Drilling Program, College Station, TX, pp. 571–586.

Narbonne, G.M., Kaufman, A.J., Knoll, A.H., 1994. Integrated carbon isotope and biostratigraphy of the upper Windemere Group, MacKenzie Mountains, NW Territories, Canada. Geol. Soc. Am. Bull. 106, 1281–1292.

Nohara, M., Ishizuka, T., Gieskes, J.M., 1984. Organic carbon isotopic composition in Cretaceous sediments, Angola Basin, Southeastern Atlantic, Deep Sea Drilling Project site 530. In: Hay, W.W., Sibuet, J.-C., et al. (Eds.), Init. Rep. DSDP, 75. U.S. Govt. Printing Office, WA, pp. 1051–1054.

Patton, J.W., Choquette, P.W., Guennel, G.K., Kaltenback, A.J., Moore, A., 1984. Organic geochemistry and sedimentology of lower to mid-Cretaceous deep-sea carbonates, sites 535 and 540, Leg 77. In: Bufler, R.T., Schlager, W., et al. (Eds.), Init. Rep., DSDP, 77. U.S. Govt. Printing Office, WA, pp. 417–443.

Pelechaty, S.M., Kaufman, A.J., Grotzinger, J.P., 1996. Evaluation of δ^{13}C isotope stratigraphy for intrabasinal correlation: data from Vendian strata of the Olenek uplift and Kharaulakh Mountains, Siberian platform, Russia. Geol. Soc. Am. Bull. 108, 992–1003.

Popp, B.N., Takigiku, R., Hayes, J.M., Lauda, J.W., Baker, E.W., 1989. The post-Paleozoic chronology and mechanism of ^{13}C depletion in primary organic matter. Am. J. Sci. 289, 436–454.

Popp, B.N., Laws, E.A., Bidigare, R.R., Dore, J.E., Hanson, K.L., Wakeham, S.G., 1998. Effect of phytoplankton cell geometry on carbon isotopic fractionation. Geochim. Cosmochim. Acta 62, 69–77.

Rau, G.H., Riebesell, U., Wolf-Gladrow, D., 1997. CO_{2aq}-dependent photosynthetic ^{13}C fractionation in the ocean: a model versus measurements. Global Biogeochemical Cycles 11, 267–278.

Raven, J.A., 1991. Physiology of inorganic C acquisition and implications for resource use efficiency by marine phytoplankton: relation to increased CO_2 and temperature. Plant Cell Environ. 14, 774–794.

Raymo, M.E., 1997. Carbon cycle models: how strong are the constraints? In: Ruddiman, W.F. (Ed.), Tectonic Uplift and Climate Change. Plenum, New York, pp. 367–381.

Romankevich, E.A., Nesterova, M.P., Shadsky, I.P., Grinchenko, A.I., 1980. Carbon and its isotopic composition in Pacific Ocean bottom sediments, Leg 56, Deep Sea Drilling Project. Scientific Party, Init. Rep. DSDP, 56, 57, Pt. 2. U.S. Govt. Printing Office, WA, pp. 1313–1317.

Saylor, B.Z., Kaufman, A.J., Grotzinger, J.P., Urban, F.E., in press. The partitioning of terminal Neoproterozoic time: constraints from Namibia. J. Sediment. Res.

Schorno, K.S., 1980. Geochemistry of carbon: Legs 56 and 57, Deep Sea Drilling Project. Scientific Party, Init. Rep. DSDP, 56, 57, Pt. 2. U.S. Govt. Printing Office, WA, pp. 1319–1325.

Schorno, K.S., Erdman, J.G., 1980. Geochemisry of carbon: Deep Sea Drilling Project sites 415 and 416. In: Lancelot, Y., Winterer, E.L., et al. (Eds.), Init. Rep. DSDP, 50. U.S. Govt. Printing Office, WA, pp. 625–627.

Shackleton, N.J., 1987. The carbon isotopic record of the Cenozoic: history of organic carbon burial and of oxygen in the ocean and atmosphere. In: Brooks, J., Fleet, A.J. (Eds.), Marine Petroleum Source Rocks. Geological Society Special Publication No. 26, Blackwell, Oxford, pp. 423–434.

Simoneit, B.R.T., Mazurek, M.A., 1981. Organic geochemistry of sediments from the Southern California Borderland, Deep Sea Drilling Project leg 63. In: Yeats, R.S., Haq, B.U., et al. (Eds.), Init. Rep. DSDP, 63. U.S. Govt. Printing Office, WA, pp. 837–853.

Simoneit, B.R.T., Philp, R.P., Jenden, P.D., Galimov, E.M., 1984. Organic geochemistry of the Deep Sea Drilling Project sediments from the Gulf of California — hydrothermal effects on unconsolidated diatom ooze. Org. Geochem. 7, 173–205.

Smith, L.H., Kaufman, A.J., Knoll, A.H., Link, P.K., 1994. Chemostratigraphy of predominantly siliciclastic Neoproterozoic successions: a case study of the Pocatello Formation and Lower Brigham Group, Idaho, USA. Geol. Mag. 131, 301–314.

Spero, H.J., Bijma, J., Lea, D.W., Bemis, B.E., 1997. Effect of seawater carbonate concentration on foraminiferal carbon and oxygen isotopes. Nature 390, 497–500.

Strauss, H., DesMarais, D.J., Hayes, J.M., Summons, R.E., 1992. The carbon-isotopic record. In: Schopf, J.W., Klein, C. (Eds.), The Proterozoic Biosphere, a Multidisciplinary Study. Cambridge Univ. Press, Cambridge, UK, pp. 117–128.

Thompson, K.F.M., Dow, W.G., 1990. Investigation of Cretaceous and Tertiary Kerogens in sediments of the Weddell Sea. In: Barker, P.F., Kennett, J.P., et al. (Eds.), Proc. ODP, Sci. Results, 113. Ocean Drilling Program, College Station, TX, pp. 189–197.

Veizer, J., Ala, D., Azmy, K, Bruckschen, P., Buhl, D., Bruhn, F., Carden, G.A.F., Diener, A., Ebneth, S., Godderis, Y., Jasper, T., Korte, C., Pawellek, F., Podlaha, O.G., Strauss, H., this volume. ^{87}Sr/^{86}Sr, δ^{13}C and δ^{18}O evolution of Phanerozoic seawater. Chem. Geol.

Welte, D.H., Kalkreuth, W., Hoefs, J., 1975. Age-trend in carbon isotopic composition in Paleozoic sediments. Naturwissenschaften 62, 482–483.

Young, G.C., Laurie, J.R., 1996. An Australian Phanerozoic Timescale. Oxford University Press, Australia, Melbourne.